Article

The Amide Rotational Barriers in Picolinamide and Nicotinamide: NMR and ab Initio Studies

Ryan A. Olsen, Lisa Liu, Nima Ghaderi, Adam Johns, Mary E. Hatcher, and Leonard J. Mueller

J. Am. Chem. Soc., **2003**, 125 (33), 10125-10132• DOI: 10.1021/ja028751j • Publication Date (Web): 24 July 2003

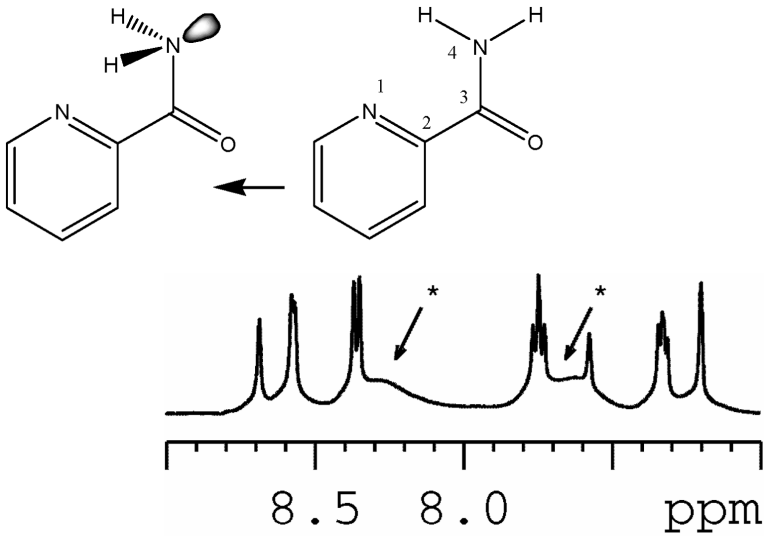

More About This Article

Additional resources and features associated with this article are available within the HTML version:

- Supporting Information
- Links to the 6 articles that cite this article, as of the time of this article download
- Access to high resolution figures
- Links to articles and content related to this article
- Copyright permission to reproduce figures and/or text from this article

View the Full Text HTML

J|A|C|S
ARTICLES
Published on Web 07/24/2003

The Amide Rotational Barriers in Picolinamide and Nicotinamide: NMR and ab Initio Studies

Ryan A. Olsen,[†] Lisa Liu,[‡] Nima Ghaderi,[†] Adam Johns,[§] Mary E. Hatcher,[⊥] and Leonard J. Mueller*,[†]

Contribution from the Department of Chemistry, University of California, Riverside, Riverside, California 92521, Scripps College, Claremont, California 91711, Claremont McKenna College, Claremont, California 91711, and W. M. Keck Science Center, The Claremont Colleges, Claremont, California 91711

Received September 30, 2002; E-mail: Leonard.Mueller@ucr.edu

Abstract: Pyridine carboxamides are a class of medicinal agents with activity that includes the reduction of iron-induced renal damage, the regulation of nicotinamidase activity, and radio- and chemosensitization. Such pharmacological activities, and the prevalence of the carboxamide moiety and the importance of amide rotations in biology, motivate detailed investigation of energetics in these systems. In this study, we report the use of dynamic nuclear magnetic resonance to measure the amide rotational barriers in the pyridine carboxamides picolinamide and nicotinamide. The activation enthalpies and entropies of $\Delta H^{\ddagger} = 12.9 \pm 0.3$ kcal/mol and $\Delta S^{\ddagger} = -7.7 \pm 0.9$ cal/mol K for nicotinamide and $\Delta H^{\ddagger} = 18.3 \pm 0.4$ kcal/mol and $\Delta S^{\ddagger} = +1.3 \pm 1.0$ cal/mol K for picolinamide report a substantial energetic difference for these regioisomers. Ab initio calculations of the rotational barriers are in good agreement with the experimentally determined values and help partition the 5.4 kcal/mol enthalpy difference into its major contributions. Of principal importance are the variations in steric interactions in the ground states of picolinamide and nicotinamide, superior π electron donation from the pyridine ring in the transition state of nicotinamide, and an intramolecular hydrogen bond in the ground state of picolinamide.

Introduction

Amides are well known to have a higher barrier to C−N bond rotation than other amines due to the partial double bond character of the amide linkage. By assuming sp^2 hybridization, the amide nitrogen can donate its lone pair electron density to the polarized carbonyl group. This favorable interaction is lost as the amide bond rotates, raising the barrier to 18 kcal/mol in the case of formamide.[1] The biological and chemical significance of amides and this intriguing partial double bond have made amide derivatives of substantial experimental and theoretical interest.[1−16] A number of studies have investigated the role of C- and N-substitutions, which result in both steric and electronic perturbations to the formamide rotational potential energy surface. Here we report on two pyridine carboxamides, the regiosiomers picolinamide (2-pyridinylcarboxamide) and nicotinamide (3-pyridinylcarboxamide, vitamin B_3) (Scheme 1). This family of compounds shows important biological activity,[17−23] with nicotinamide adenine dinucleotide (NAD) playing a crucial role in biological oxidative chemistry. Nicotinamide and picolinamide also serve as model compounds for the conformations of polypeptides and nucleic acids,[24,25] and the amide groups in picolinamide and nicotinamide can adopt a variety of tautomeric and rotameric structures in addition to forming interesting molecular associations via hydrogen bond-

[†] University of California, Riverside.
[‡] Scripps College.
[§] Claremont McKenna College.
[⊥] W. M. Keck Science Center.

(1) Taha, A.; True, N. *J. Phys. Chem. A* **2000**, *104*, 2985−2993.
(2) Stewart, W. E.; Siddall, T. H. *Chem. Rev.* **1970**, *70*, 517−551.
(3) Rabinovitz, M.; Pines, A. *J. Am. Chem. Soc.* **1969**, *91*, 1585.
(4) Bain, A. D.; Hazendonk, P.; Couture, P. *Can. J. Chem.* **1999**, *77*, 1340−1348.
(5) Fontoura, L. A. M.; da Cruz Rigotti, I. J.; Correia, C. R. D. *J. Mol. Struct.* **2002**, *609*, 73−81.
(6) Wiberg, K. B.; Laidig, K. E. *J. Am. Chem. Soc.* **1987**, *109*, 5935.
(7) Wiberg, K. B.; Breneman, C. M. *J. Am. Chem. Soc.* **1992**, *114*, 831.
(8) Wiberg, K. B.; Hadad, C. M.; Rablen, P. R.; Cioslowski, J. J. *J. Am. Chem. Soc.* **1992**, *114*, 8644.
(9) Wiberg, K. B.; Rablen, P. R.; Rush, D. J.; Keith, T. A. *J. Am. Chem. Soc.* **1995**, *117*, 4261.
(10) Fogarasi, G.; Szalay, P. G. *J. Phys. Chem. A* **1997**, *101*, 1400.
(11) Basch, H.; Shmaryahu, H. *Chem. Phys. Lett.* **1998**, *294*, 117.
(12) Bennet, A. J.; Wang, Q. P.; Slebocka-Tilk, H.; Somayaji, R. S.; Brown, R. S.; Santarsiero, B. D. *J. Am. Chem. Soc.* **1990**, *112*, 6383.
(13) Fisher, G. *Chem. Soc. Rev.* **2000**, *29*, 119−127.
(14) Campomanes, P.; Menendez, M. I.; Sordo, T. L. *J. Phys. Chem. A* **2002**, *106*, 2623−2628.
(15) Cox, C.; Lectka, T. *J. Org. Chem.* **1998**, *63*, 2426−2427.
(16) Berg, U.; Astrom, N. *Acta Chem. Scand.* **1995**, *49*, 599−608.
(17) Taguchi, H. *Furi Rakijaru no Rinsho* **1999**, *14*, 23−28.
(18) Pero, R. W.; Olsson, A.; Amiri, A.; David, C. *Cancer Detect. Prev.* **1998**, *22*, 225−236.
(19) Kawabata, T.; Ogino, T.; Mori, M.; Awai, M. *Acta Pathol. Jpn.* **1992**, *42*, 469−475.
(20) Ogata, S.; Takeuchi, M.; Teradaira, S.; Yamamoto, N.; Iwata, K.; Okumura, K.; Taguchi, H. *Biosci. Biotechnol. Biochem.* **2002**, *66*, 641−645.
(21) Ogata, S.; Takeuchi, M.; Fujita, H.; Shibata, K.; Okumura, K.; Taguchi, H. *Biosci. Biotechnol. Biochem.* **1998**, *62*, 2351−2356.
(22) Shimai, T.; Islam, T.; Fukushi, Y.; Hashidoko, Y.; Yokosawa, R.; Tahara, S. *Z. Naturforsch.* **2002**, *57*, 323−331.
(23) Sarma, R. H.; Woronick, C. L. *Biochemistry* **1972**, *11*, 170−179.
(24) Singa, N. C.; Sathyanarayana, D. N. *Spectrochim. Acta Part A* **1998**, *54*, 1059−1065.
(25) Takano, T.; Sasada, Y.; Kakudo, M. *Acta Crystallogr.* **1966**, *21*, 514−522.

10.1021/ja028751j CCC: $25.00

Scheme 1

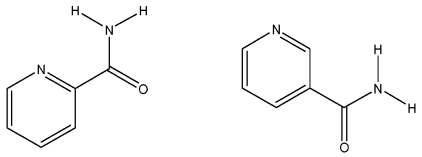

ing.[25,26] As well, picolinamide introduces a novel twist in the carboxamide potential by its ability to form an intramolecular hydrogen bond between the amide and the pyridine ring.[24,25,27] This hydrogen bond should have significant effects on the rotational barrier, but to date no values for the barriers have been reported for any of the pyridine carboxamides.

Here we present experimental measurements of the rotational barriers in picolinamide and nicotinamide as determined by dynamic nuclear magnetic resonance (NMR) spectroscopy.[28,29] As the amide bond rotates, the chemically inequivalent nitrogen protons exchange. The resulting dynamic NMR spectra are quite sensitive to the rate of this exchange and provide a powerful and well-established method for extracting the kinetic parameters through variable-temperature NMR experiments. These experiments show a markedly higher activation energy for bond rotation in picolinamide than in nicotinamide. Ab initio calculations for the ground and transitions states suggest that the following three factors are most important in differentiating the amide rotational barriers in nicotinamide and picolinamide: (1) a hydrogen bond between the amide proton and the pyridine nitrogen in the ground state of picolinamide; (2) steric interactions in the ground state of nicotinamide; and (3) superior π electron donation from the pyridine ring to the carbonyl in the transition state of nicotinamide. These effects are additive, raising the barrier in picolinamide and lowering it in nicotinamide. A thorough understanding of these contributions helps shed light on the structural and electronic factors responsible for the differential pharmacological activity of these two compounds.

Materials and Methods

^{1}H NMR spectra were recorded on a Bruker DMX400 spectrometer (^{1}H frequency 400.13 MHz) equipped with a 5 mm high-resolution double resonance probe with the second channel tuned for ^{14}N decoupling. Spectra were acquired over a range of temperatures from −20 to 150 °C via a Bruker BVT-3300 digital variable-temperature control unit. Samples of nicotinamide (Aldrich) and picolinamide (Aldrich) were prepared in deuterated pyridine and nitrobenzene (Cambridge) at 5 mg/mL and placed in the inner portion of a 5 mm/3 mm (o.d.) double NMR tube (Wilmad). The outer tube was filled with ethylene glycol (Aldrich) for temperature calibration.[30] A rough estimate of the temperature was provided by the probe thermocouple, while the actual temperature was determined using the ethylene glycol chemical shift thermometer in thermal contact with the sample. This method was found to provide the most accurate temperature reading for the sample, and the probe thermocouple deviated from this reading by as much as 10 °C at higher temperatures. The choice of pyridine and nitrobenzene as solvents was made on the basis of their abilities to accept hydrogen bonds and their convenient liquid-phase temperature range. Aqueous solutions were avoided due to exchange between the amide protons and the water molecules.

A one-pulse experiment with CYCLOPS phase cycling[31] and inverse-gated ^{14}N decoupling was used to obtain one-dimensional NMR data. The ^{14}N decoupling suppressed magnetization transfer from the proton to the quickly relaxing quadrupolar ^{14}N nucleus and resulted in a narrowing of the slow-exchange amide proton lines by 4−5 Hz.

Conformer exchange rates were extracted using complete line shape analysis [32] in a simulation program written within the Mathematica programming environment.[33] The unified Liouvillian approach of Binsch[32] was used to solve the spin dynamics for the equivalent exchange of the two amide protons and to generate the resulting NMR spectrum. This method takes into account both spin evolution under a general NMR Hamiltonian and kinetic exchange of the NMR active nuclei. As the majority of the data were acquired in the slow- and intermediate-exchange regimes, no attempt was made to quantify the recently identified quantum statistical contributions to the dynamic NMR spectral parameters.[34] Input parameters to the Liouvillian dynamics were the two resonance line positions, their amplitude, the effective transverse relaxation constant (T_2*), and the exchange rate. A model consisting of the exchanging peaks, a number of nonexchanging peaks (used to accommodate spectral overlap in the fit window), and a quadratic baseline correction was then fit to the experimental spectrum in a nonlinear least-squares manner.[35] In the few cases of extreme spectral overlap in which this fitting procedure failed, one of the exchange peaks was typically unobscured. These cases were handled by fixing the chemical shift difference between the exchanging peaks at the experimentally observed value and fitting only the spectral region of the one peak. In each fit, all parameters were free to vary except T_2*, which was fixed by experimental measurement in slow exchange. As the extracted kinetic rates came mostly from the slow-exchange regime where T_2* was known most accurately and from intermediate exchange where the rates were not as dependent on this parameter, T_2* was assumed to be constant with temperature.

The extracted rates were used to characterize the barrier to amide bond rotation as an entropy and enthalpy of activation according to transition state theory.[36] Nonlinear least-squares fitting of the rate data was again performed in Mathematica, with the data weighted inversely proportional to the rate. This weighting was determined empirically by noting the variation of the fit residuals for the kinetic data. Under exchange, the observed line shapes depend strongly on the kinetic rate and the chemical shift difference between the exchanging peaks. Because of the large temperature dependence observed for the amide chemical shifts, only rate data from the slow-exchange and the start of intermediate-exchange regions were considered reliable. Error bars for the transition state parameters were determined through a numerical calculation of the covariance matrix and are reported as ± one standard error.[35]

(26) Katritzky, A. R.; Ghiviriga, I. *J. Chem. Soc., Perkin Trans. 2: Phys. Org. Chem.* **1995**, *8*, 1651−1653.
(27) Anad, J.; Singha, N. C.; Sathyanarayana, D. N. *J. Mol. Struct.* **1997**, *412*, 221−229.
(28) Sandstrom, J. *Dynamic NMR Spectroscopy*; Academic Press: London, 1982.
(29) Jackman, L. M.; Cotton, F. A. *Dynamic Nuclear Magnetic Resonance Spectroscopy*; Academic Press: New York, 1975.
(30) Raiford, D. S.; Fisk, C. L.; Becker, E. D. *Anal. Chem.* **1979**, *51*, 2050−2051.
(31) Hoult, D. I.; Richards, R. E. *Proc. R. Soc. (London)* **1975**, *A344*, 311.
(32) Binsch, G. *J. Am. Chem. Soc.* **1969**, *91*, 1304.
(33) Wolfram, S. *Mathematica: A System for Doing Mathematics by Computer*, 2nd ed.; Addison-Wesley Publishing Co.: Reading, MA, 1991.
(34) Mueller, L. J.; Weitekamp, D. P. *Science* **1999**, *283*, 61−65.
(35) Press: W. H.; Teukolsky, S. A.; Vetterling, W. T.; Flannery, B. P. *Numerical Recipes in C: the Art of Scientific Computing*, 2nd ed.; Cambridge University Press: Cambridge, 1992.
(36) Pechukas, P. *Annu. Rev. Phys. Chem.* **1981**, *32*, 159−177.
(37) Frisch, M. J.; Trucks, G. W.; Schlegel, H. B.; Scuseria, G. E.; Robb, M. A.; Cheeseman, J. R.; Zakrzewski, V. G.; Montgomery Jr., J. A.; Stratmann, R. E.; Burant, J. C.; Dapprich, S.; Millam, J. M.; Daniels, A. D.; Kudin, K. N.; Strain, M. C.; Farkas, O.; Tomasi, J.; Barone, V.; Cossi, M.; Cammi, R.; Mennucci, B.; Pomelli, C.; Adamo, C.; Clifford, S.; Ochterski, J.; Petersson, G. A.; Ayala, P. Y.; Cui, Q.; Morokuma, K.; Malick, D. K.; Rabuck, A. D.; Raghavachari, K.; Foresman, J. B.; Cioslowski, J.; Ortiz, J. V.; Baboul, A. G.; Stefanov, B. B.; Liu, G.; Liashenko, A.; Piskorz, P.; Komaromi, I.; Gomperts, R.; Martin, R. L.; Fox, D. J.; Keith, T. A.; Al-Laham, M. A.; Peng, C. Y.; Nanayakkara, A.; Challacombe, M.; Gill, P. M. W.; Johnson, B.; Chen, W.; Wong, M. W.; Andres, J. L.; Gonzalez, C.; Head-Gordon, M.; Replogle, E. S.; Pople, J. A. *Gaussian 98*, Revision A.9; Gaussian, Inc.: Pittsburgh, PA, 1998.

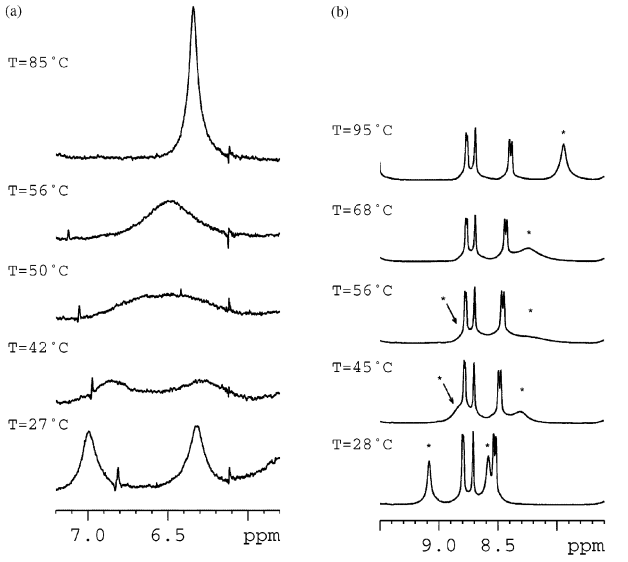

Figure 1. Dynamic NMR spectra of nicotinamide in (a) nitrobenzene and (b) pyridine solvents over a range of temperature. Only the spectral region of the amide protons is shown in (a), while these protons are denoted by asterisks in (b). Under chemical exchange, the spectral lines broaden and then coalesce into a single peak. In this regime, the line shapes are a sensitive function of the exchange rate.

Ab initio calculations were performed at the Hartree−Fock, MP2 electron correlation,[35] and density functional (DFT) levels of theory using the Gaussian 98 software package.[37] For each level of theory, molecules were optimized without constraint to their ground and transition state geometries using the 6-31G(d,p) basis[38] with corresponding single-point energies calculated with the 6-311++G(d,p) basis. Ground and transition states were verified by frequency analysis after optimization and zero-point energy corrections applied with the appropriate scaling.[39,40] For density functional calculations, the B3LYP functional was chosen.[41−43] The Fermi contact contribution to the scalar couplings[44−46] was also calculated in Gaussian 98 using DFT/finite perturbation theory (FPT) methods,[47−49] the unrestricted B3LYP functional, and the 6-311++G(d,p) basis.

Results and Discussion

As the amide bond rotates, chemical exchange of the two amide protons has a profound effect on the observed NMR line shapes. Figures 1 and 2 show the ^{1}H NMR spectra of picolinamide and nicotinamide at different temperatures and under different rates of chemical exchange. In the limit of slow exchange (lower temperature), distinct resonances are observed for the amide protons (labeled with asterisks). The chemical shifts of the amide protons differ most significantly for

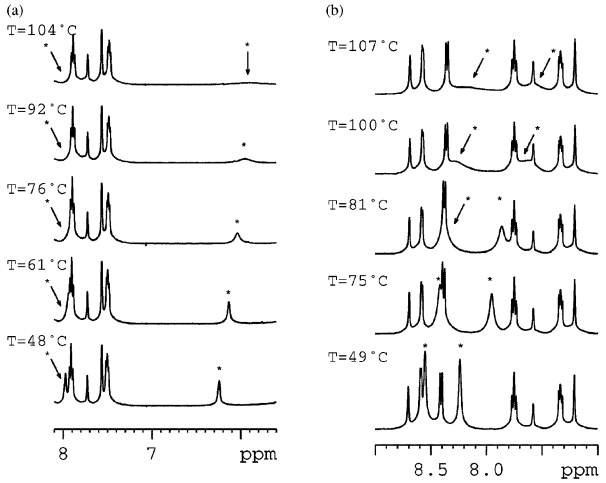

Figure 2. Dynamic NMR spectra of picolinamide in (a) nitrobenzene and (b) pyridine solvents as a function of temperature. The amide protons are denoted by asterisks.

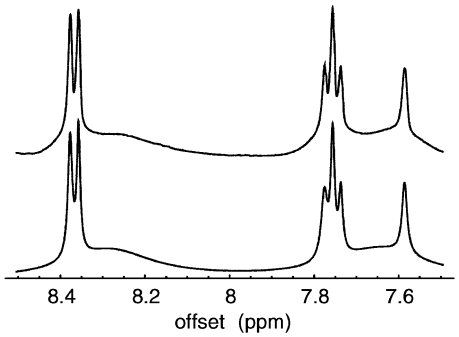

Figure 3. Example of fitting the dynamic NMR spectrum of picolinamide in the solvent pyridine at 100 °C. The experimental data (top) are modeled (bottom) using complete line shape analysis of the exchanging peaks and several additional peaks to accommodate the spectral overlap.

picolinamide in nitrobenzene, and the downfield-shifted proton suggests an intramolecular hydrogen bond.[50]

As the temperature rises and the exchange rate increases, the lines broaden and eventually coalesce. It is in this region that the line shapes depend most sensitively on rate. For picolinamide, coalescence occurs close to 120 °C, while for nicotinamide it occurs near 50 °C. This temperature difference reports a significantly larger barrier to amide rotation in picolinamide. Complete line shape analysis of the exchanging peaks provides a quantitative measure of the rates. Although many of the spectra contain overlapping resonances, the precision of the extracted rates is not significantly compromised, and Figure 3 shows an example of the quality of the fits. Plots of the rate versus temperature extracted by complete line shape analysis for both compounds are shown in Figure 4, and the rates are listed in Table 1.

The barrier to bond rotation is interpreted using transition state theory,[36] with the rate related to the enthalpy and entropy of activation by

$$k = \frac{k_B T}{h} e^{\Delta S^{\ddagger}/R} e^{-\Delta H^{\ddagger}/RT}$$

Here k_B is the Boltzmann constant, h is Planck's constant, and

(38) Hehre, W. J.; Radom, L.; Schleyer, P. v. R.; Pople, J. A. *Ab Initio Molecular Orbital Theory*; Wiley: New York, 1986.
(39) El-Azhary, A. A.; Suter, H. U. *J. Phys. Chem.* **1996**, *100*, 15056.
(40) Pople, J. A.; Schlegel, H. B.; Krishnan, R.; Defrees, D. J.; Binkley, J. S.; Frisch, M. J.; Whiteside, R. A.; Hout, R. F.; Hehre, W. *J. Int. J. Quantum Chem. Symp.* **1981**, *15*, 269.
(41) Becke, A. D. *Phys. Rev. A* **1988**, *38*, 3098.
(42) Becke, A. D. *J. Chem. Phys.* **1993**, *98*, 5648.
(43) Lee, C.; Yang, W.; Parr, R. G. *Phys. Rev. B* **1988**, *37*, 785.
(44) Pecul, M.; Leszczynski, J.; Sadlej, J. *J. Chem. Phys.* **2000**, *112*, 7930.
(45) Fierman, M.; Nelson, A.; Khan, S. I.; Barfield, M.; O'Leary, D. J. *Org. Lett.* **2000**, *2*, 2077.
(46) Benedict, H.; Shenderovich, I. G.; Malkina, O. L.; Malkin, V. G.; Denisov, G. S.; Golubev, N. S.; Limbach, H. H. *J. Am. Chem. Soc.* **2000**, *122*, 1979.
(47) Pople, J. A.; McIver, J. W., Jr.; Ostlund, N. S. *J. Chem. Phys.* **1968**, 2960.
(48) Onak, T.; Jaballas, J.; Barfield, M. J. *J. Am. Chem. Soc.* **1999**, *121*, 2850.
(49) Barfield, M.; Dingley, A. J.; Feigon, J.; Grzesiek, S. *J. Am. Chem. Soc.* **2001**, *123*, 4014.
(50) Szczepura, L. F.; Eilts, K. K.; Hermetet, A. K.; Ackerman, L. J.; Swearingen, J. K.; West, D. X. *J. Mol. Struct.* **2002**, *607*, 101−110.

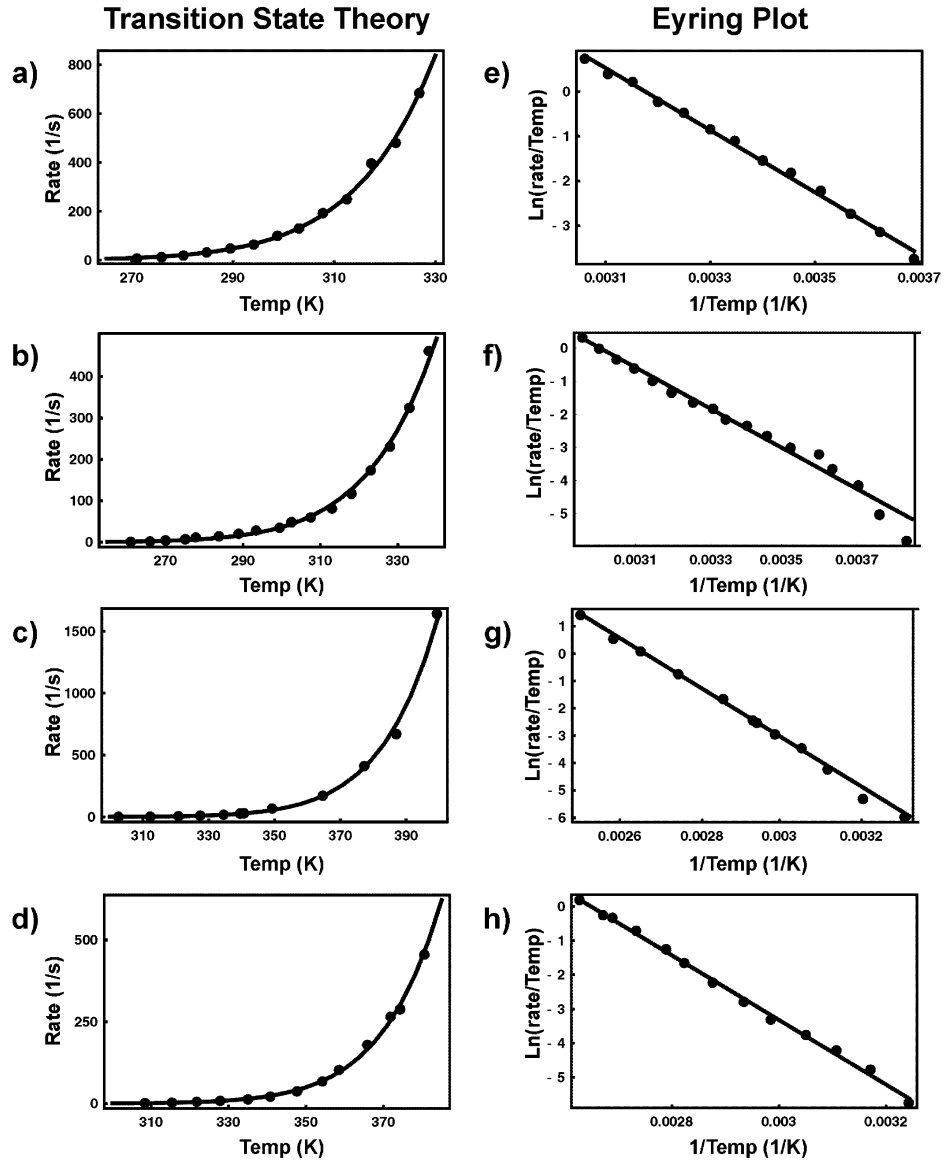

Figure 4. Temperature dependence of the exchange rate for nicotinamide in (a, e) nitrobenzene and (b, f) pyridine and picolinamide in (c, g) nitrobenzene and (d, h) pyridine solvents allows for the extraction of the enthalpy and entropy of activation according to transition state theory. Best fits for the activation parameters (Table 2) are shown as the solid lines for both the direct fit of the rate vs temperature data (a−d) and the Eyring plots of the data (e−h).

the other symbols have their usual meanings. The best fits from transition state theory are summarized in Table 2 and are shown as the solid lines in Figure 4. The best-fit averages of $\Delta H^{\ddagger} = 12.9 \pm 0.3$ kcal/mol and $\Delta S^{\ddagger} = -7.7 \pm 0.9$ cal/mol K for nicotinamide and $\Delta H^{\ddagger} = 18.3 \pm 0.4$ kcal/mol and $\Delta S^{\ddagger} = +1.3 \pm 1.0$ cal/mol K for picolinamide report a substantial difference of 5.4 kcal/mol in the activation enthalpies. For comparison, we also present the data in terms of the Eyring plot of ln k/T versus $1/T$ in Figure 4. This is a popular way to present kinetic data in NMR, and the linear least-squares best fit of the data gives values similar to the direct nonlinear least-squares fit for the activation enthalpy and entropy (Table 2).

Several points are worth noting with respect to fitting the rate data. To begin, errors in the best-fit entropy and enthalpy are highly correlated. Specifically, a systematic error that raises the value of one fit parameter will also raise the other in a manner that keeps the free energy approximately constant. Second, the fitting procedure is particularly sensitive to small systematic errors in the slow-exchange line width as parametrized by T_2*. Errors in T_2* essentially shift the extracted slow-exchange rates by a constant value, which alters the best-fit entropy and enthalpy of activation. For example, if the slow-exchange T_2* is varied by ±10%, variations in the best-fit enthalpy and entropy of $\Delta H^{\ddagger} = 1$ kcal/mol and $\Delta S^{\ddagger} = 10$ cal/mol K, respectively, are observed. This strong dependence of the fit parameters on slow-exchange line width is highly undesirable, as the slow-exchange line width is not always characterized to within this level of accuracy. Constant errors in the rate can be identified as a constant in the rate versus temperature profile or as a nonlinear component in the Eyring plot of ln k/T versus $1/T$. Correcting a constant systematic error is difficult in rate data, being essentially the ill-posed problem of fitting a compound curve that is the sum of two exponentials[51,52] in the former case. For Eyring plots, Bain and

(51) Jericevic, Z.; Benson, D. M.; Bryan, J.; Smith, L. C. *Anal. Chem.* **1987**, *59*, 658−662.
(52) Knutson, J. R.; Beechem, J. M.; Brand, L. *Chem. Phys. Lett.* **1983**, *102*, 501−507.

Table 1. Experimental Data for Amide Bond Rotation

nicotinamide in nitrobenzene		nicotinamide in pyridine		picolinamide in nitrobenzene		picolinamide in pyridine	
T (K)	rate (1/s)	*T* (K)	rate (1/s)	*T* (K)	rate (1/s)	*T* (K)	rate (1/s)
271.0	6.4	261.0	0.8	302.6	0.8	308.4	1.0
275.9	11.8	266.0	1.7	312.2	1.5	315.4	2.7
280.2	18.1	270.0	4.2	320.8	4.6	321.8	4.8
284.8	30.8	275.1	7.1	327.4	10.3	327.9	7.6
289.5	46.9	277.8	11.2	334.6	17.4	335.0	12.2
294.1	62.8	283.8	13.9	339.6	27.2	340.8	20.8
298.8	98.9	288.9	20.2	340.7	29.4	347.7	37.3
303.0	129.8	293.4	28.0	349.3	66.5	354.2	67.3
307.8	192.0	299.5	34.4	364.7	171.6	358.5	102.2
312.5	249.0	302.6	48.4	377.3	409.5	365.8	178.7
317.3	395.5	307.5	59.3	387.0	668.4	371.9	265.0
322.2	479.0	313.0	80.9	399.3	1640.7	374.3	288.0
326.8	684.2	318.0	116.9			380.5	454.9
		323.0	173.2				
		328.0	230.4				
		333.0	324.3				
		338.0	460.8				

Table 2. Experimental Activation Energies for Amide Bond Rotation Using Three Different Methods

	direct fit		Eyring plot		derivative	
	$\Delta H^{\ddagger a}$	$\Delta S^{\ddagger b}$	$\Delta H^{\ddagger a}$	$\Delta S^{\ddagger b}$	$\Delta H^{\ddagger a}$	$\Delta S^{\ddagger b}$
nicotinamide						
in nitrobenzene	13.1 ± 0.3	-5.8 ± 0.8	13.8 ± 0.3	-3.3 ± 0.8	12.9 ± 1.2	-6.2 ± 3.7
in pyridine	12.6 ± 0.3	-9.5 ± 1.0	12.4 ± 0.5	-10.0 ± 1.7	12.3 ± 1.0	-10.0 ± 2.9
picolinamide						
in nitrobenzene	17.9 ± 0.4	0.4 ± 1.0	18.4 ± 0.4	1.7 ± 1.0	18.6 ± 1.2	2.0 ± 3.1
in pyridine	18.6 ± 0.4	2.2 ± 1.0	18.8 ± 0.3	2.5 ± 0.8	18.8 ± 0.6	2.7 ± 1.7

[a] Energy in kcal/mol. [b] Entropy in cal/mol K.

co-workers[53] have also shown how the first few rate points can skew the best-fit entropy and lead to substantial systematic errors. We have developed an alternate method for treating the rate data that removes the sensitivity of the fit parameters to the slow-exchange T_2* by fitting the derivative of the rate versus temperature data. While taking the derivative unfortunately increases the noise in the data, the extracted best-fit activation parameters are found to be completely insensitive to a constant systematic error in the initial rates and T_2*. In Figure 5, the best fits to the derivative data for the enthalpy and entropy of activation are shown. These fits again agree well with the direct fits in Figure 4 and are tabulated in Table 2.

The higher barrier to rotation for picolinamide supports the role of an intramolecular hydrogen bond, although ab initio calculations point to several features that distinguish the potentials. Structurally, ab intio calculations show substantial differences between picolinamide and nicotinamide in both their ground and transition states. Scheme 2 reports the two lowest energy ground states and four lowest energy pathways for amide bond rotation that were found for both molecules. As in the case of other amides, the ground states exhibit a roughly planar geometry for the amide nitrogen, while the nitrogens are pyramidalized in the transition states. The planar geometry allows for delocalization of π electrons between the carbonyl and amide nitrogen. In GSP1 for picolinamide, the molecule is completely planar with one of the amide protons directly in front of the pyridine nitrogen. In the case of GSP2 and both of the ground states of nicotinamide (GSN1 and GSN2) there is a twist of the amide plane from that of the pyridine ring due to steric interactions with the ring protons. There are also slight deviations from planarity at the amide nitrogen in nicotinamide. The transition states for the molecules are very similar in structure, with only slight deviations in the amide region. Table 3 summarizes the geometric data.

The ab initio energies characterizing the gas-phase rotational barriers in Scheme 2 are detailed in Table 4. The molecular energies are measured relative to the lowest energy ground state for each molecule. For picolinamide, GSP2 is much higher in energy than GSP1, making its population at room temperature of little consequence. The reaction pathway through GSP2 and TSP2′, however, is competitive with the reaction pathway through TSP1′. The preferred pathway for picolinamide, however, is through TSP1, which has both of the amide protons pointing back to the pyridine ring. For nicotinamide there is only a slight energetic difference between GSN1 and GSN2, and we presumably observe a fast-exchange average over the two populations at all experimental temperatures. The amide proton exchange may also proceed equally fast from either ground state through TSN1′ or TSN2′. These lowest energy transition states for nicotinamide have the protons pointing away from the ring, again likely due to steric effects. Contrasting methods, the DFT calculations for all barriers are 1−2 kcal/mol higher than those for Hartree−Fock and MP2, which at 11.5 and 12.5 kcal/mol for nicotinamide and 18.2 and 18.4 kcal/mol for picolinamide are closest to the experimental results.

The ground state geometry displays a favorable arrangement for the formation of an intramolecular hydrogen bond in picolinamide. In particular, the distance between the amide proton and pyridine nitrogen is 2.304 Å, close enough for a hydrogen bond to form. NMR presents a powerful experimental tool for identifying hydrogen bonding as a scalar coupling between the donated proton and the hydrogen bond acceptor.[54] Both hydrogen bonding and scalar couplings rely on covalently shared electron density between the participants. In the absence

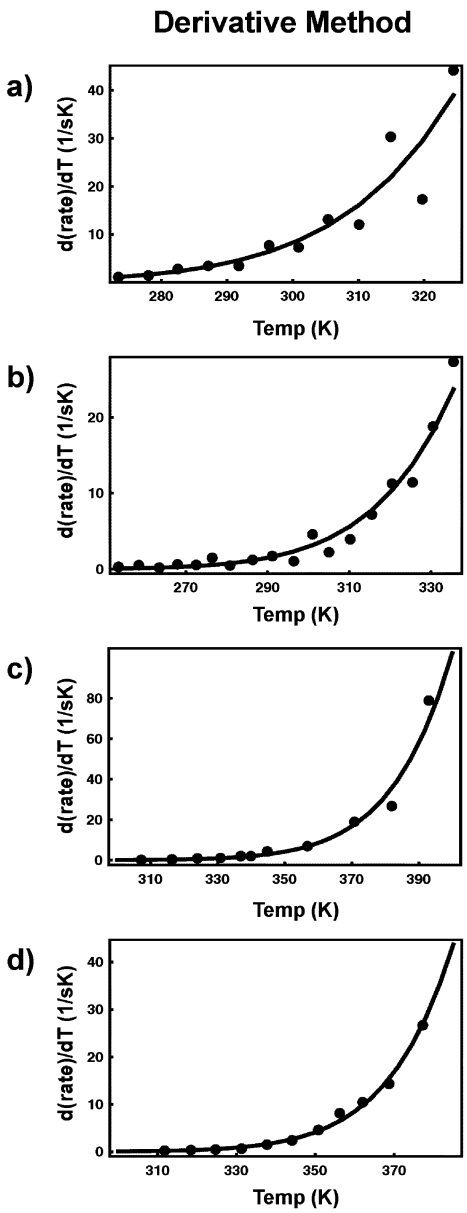

Figure 5. The alternate method of fitting the derivative of the rate data vs temperature is insensitive to systematic errors in the slow-exchange line width. Best fits for the activation parameters for nicotinamide in (a) nitrobenzene and (b) pyridine and picolinamide in (c) nitrobenzene and (d) pyridine solvents are shown as the solid lines and are tabulated in Table 2.

of ^{15}N-labeled materials, the experimental observation of the coupling is precluded. The ab initio calculation of the scalar coupling, however, is straightforward, and we make use of it here to confirm the intramolecular hydrogen bond. For scalar couplings involving protons, the Fermi contact interaction tends to be the dominant contribution[49,55] and is the only component that we consider. Calculations in Gaussian 98 give a $^{1h}J_{HN}$ scalar coupling of 1.3 Hz across the hydrogen bond for the ground state of picolinamide. In the transition state of picolinamide, the scalar coupling falls to 0.15 Hz, indicating that most of the hydrogen bond has been lost. To verify that the calculated scalar

Scheme 2

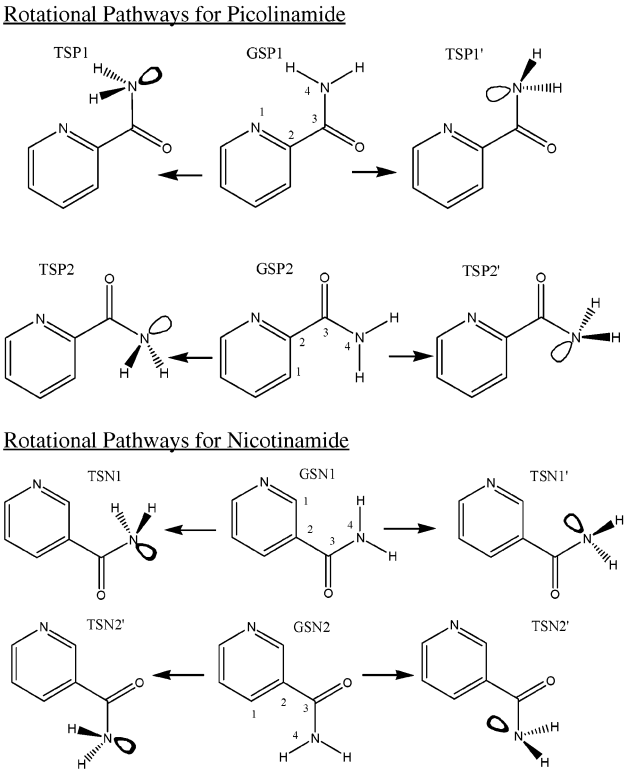

coupling is due to a hydrogen bond interaction and not a four-bond scalar coupling ($^4J_{HN}$), we also investigated the model system of ammonia and pyridine fixed in a geometry analogous to that for the amide region of picolinamide, as shown in Figure 6. In this case, only an intermolecular hydrogen bond interaction can be responsible for the calculated scalar coupling ($^{1h}J_{HN}$) of 0.54 Hz. On the basis of both the picolinamide and the model system calculations, we believe that there is strong evidence for an intramolecular hydrogen bond in the ground state of picolinamide. For a standard hydrogen bond, as is likely the case here, one would expect 2−3 kcal/mol of stabilization.[56]

The remaining gap of 2−3.5 kcal/mol in the picolinamide and nicotinamide barriers is ascribed to differences in steric interactions and π electron donation. The alternative amide resonance structures[57] for nicotinamide and picolinamide (Scheme 3) illustrate the importance of these factors. We note that for Wiberg's model,[7] analogous resonance structures could be drawn, but the oxygen would only spectate and the bond order for the carbonyl would not change substantially. In the ground state of both molecules all three resonance structures can contribute, although I and II dominate. The steric interactions in the ground state of nicotinamide are noted by the larger pyramidalization of the nitrogen and the slightly longer C−N bond (Table 3). Both imply less resonance stabilization from I, with its double bond character, and therefore a smaller barrier to rotation. In the transition state, resonance I is no longer able to contribute in either molecule and the importance of III increases. Here, nicotinamide has the distinct advantage as the positive charge is dispersed over three carbons, while picolinamide's resonance includes positive charge on the more

(53) Bain, A. D.; Duns, G. J.; Ternieden, S.; Ma, J.; Werstiuk, N. H. *J. Phys. Chem.* **1994**, *98*, 7458−7463.
(54) Dingley, A. J.; Masse, J. E.; Peterson, R. D.; Barfield, M.; Feigon, J.; Grzesiek, S. *J. Am. Chem. Soc.* **1999**, *121*, 6019−6027.
(55) Del Bene, J. E.; Perera, S. A.; Bartlett, R. J. *J. Am. Chem. Soc.* **2000**, *122*, 3560−3561.
(56) Pimentel, G. C.; McClellan, A. L. *Annu. Rev. Phys. Chem.* **1971**, *22*, 347−385.
(57) Kallies, B.; Kleinpeter, E.; Koch, A.; Mitzner, R. *J. Mol. Struct.* **1997**, *435*, 123−132.

Table 3. Optimized Molecular Parameters[a]

	dihedral angle[c] 1–2–3–4	nitrogen pyramidalization angle[c]	dipole moment[b]	C–N bond[d]	N–H1 bond[d]	N–H2 bond[d]
nicotinamide						
ground state 1	19.8	354.0	2.13	1.358	0.992	0.995
ground state 2	22.2	352.1	5.17	1.362	0.992	0.995
transition state 1	0.0	330.0	2.66	1.428	1.003	1.003
transition state 1′	0.0	320.6	0.47	1.433	1.005	1.005
transition state 2	0.0	331.3	5.42	1.426	1.001	1.001
transition state 2′	0.0	320.8	3.58	1.432	1.004	1.004
picolinamide						
ground state 1	0.0	360.0	3.14	1.342	0.993	0.994
ground state 2	41.0	352.8	5.55	1.363	0.993	0.995
transition state 1	0.0	321.9	5.11	1.422	1.005	1.005
transition state 1′	0.0	321.0	1.99	1.425	1.005	1.005
transition state 2	0.0	331.8	6.53	1.428	1.001	1.001
transition state 2′	0.0	320.9	3.93	1.434	1.004	1.004

[a] Structures optimized at HF/6-31G(d,p). [b] Dipole moments in Debyes. [c] Angles in degrees. [d] Bond lengths in angstroms.

Table 4. Calculated Rotational Barriers in kcal/mol

	ground state 1	ground state 2	rotational+ barrier 1	rotational barrier 1′	rotational barrier 2	rotational barrier 2′
nicotinamide						
HF/6-311++G(d,p)[a]	0	0.9	16.2	11.5	17.2	11.8
B3LYP/6-311++G(d,p)[b]	0	1.0	17.4	13.1	18.3	13.5
MP2/6-311++G(d,p)[a]	0	0.7	16.4	12.5	17.4	12.8
picolinamide						
HF/6-311++G(d,p)[a]	0	8.8	18.4	20.4	25.8	20.5
B3LYP/6-311++G(d,p)[b]	0	9.1	20.1	22.2	26.8	21.8
MP2/6-311++G(d,p)[a]	0	7.5	18.2	20.5	24.9	19.8

[a] Structure minimized at HF/6-31G(d,p). Corrected with zero-point energies at HF/6-31G(d,p) scaled by 0.9. [b] Structure minimized at B3LYP/6-31G(d,p). Corrected with zero-point energies at B3LYP/6-31G(d,p) scaled by 0.96.

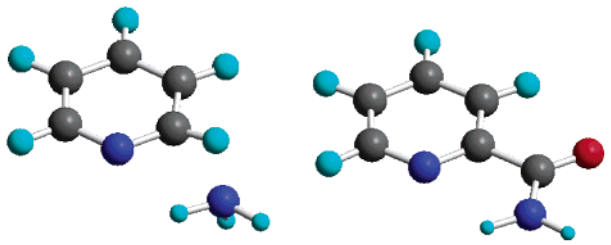

Figure 6. A model system for examining the hydrogen bond between the amide proton and the pyridine nitrogen in picolinamide (right) is ammonia and pyridine (left). In the latter case, the nitrogen and two of the protons on ammonia are fixed in the geometry for the amide group in picolinamide and the remaining proton and lone pair are minimized to a lowest energy configuration. The calculated scalar couplings to the pyridine ring nitrogen of 1.3 and −0.7 Hz, respectively, for the syn and anti protons in picolinamide are likely a mixture of through-hydrogen bond and long-range scalar couplings ($^{1h}J_{HN}$ and $^{4}J_{HN}$ for syn; $^{3h}J_{HN}$ and $^{4}J'_{HN}$ for anti). For the model system (left) the calculated scalar couplings of 0.54 and −1.3 Hz, respectively, for syn and anti and 0.1 Hz for the additional proton can only be due to a through-hydrogen bond scalar interaction. The proton that is anti does not have a zero coupling to the pyridine nitrogen in either case, indicating an important role for $^{3h}J_{HN}$.

electronegative pyridine nitrogen. Because of this unfavorable delocalization, it is unlikely that picolinamide is stabilized by resonance III to the same degree as nicotinamide. Ab initio calculations of the charge on the pyridine ring support this picture. Figure 7 shows that the pyridine ring in picolinamide actually gains electron density moving from the ground to the transition state, although part of this gain may be due to the loss of the hydrogen bond. The ring in nicotinamide, however, donates electron density to the carbonyl in the transition state, giving it a net positive change. Both the steric interactions and the resonance stabilization lower the barrier for nicotinamide

Scheme 3. Alternate Amide Resonance Structures for Picolinamide and Nicotinamide

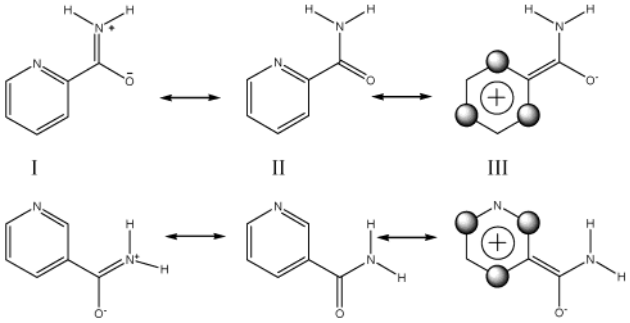

relative to picolinamide. By analogy to other amide systems,[58,59] we estimate that the slight loss of planarity at the nitrogen in the ground state of nicotinamide is responsible for ∼1 kcal/mol of this difference. This value is consistent with our calculations of the energy change in formamide as it moves from a completely planar ground state to a similar pyramidalization. The remaining 1−2 kcal/mol comes from the larger resonance stabilization of the pyridine ring in nicotinamide.

The difference in amide bond rotational barriers for nicotinamide and picolinamide reflects steric and electronic properties that also lead to significant variations in their chemical reactivity. For example, picolinamide and nicotinamide have been used as drugs to prevent iron-induced renal damage, although nicotinamide also promotes DNA damage by iron, while

(58) Sponer, J.; Hobza, P. *Int. J. Quantum Chem.* **1996**, *57*, 959−970.
(59) Bludsky, O.; Sponer, J.; Leszcynski, J.; Spirko, V.; Hobza, P. *J. Chem. Phys.* **1996**, *105*, 11042.

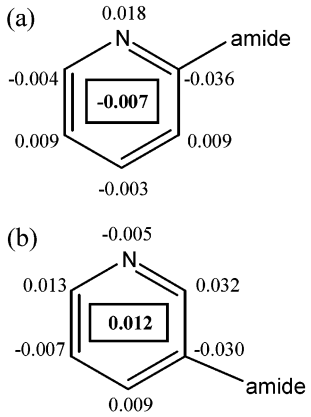

Figure 7. Change in charge for the pyridine ring in picolinamide (a) and nicotinamide (b) going from the ground to transition state. The net change is indicated by the boxed value.

picolinamide does not.[19] As well, picolinamide and other structural isomers of nicotinamide induce apoptosis in acute myelomonocytic leukemia cells (HL-60), while nicotinamide is inert.[21] A number of studies highlight additional differences between these two, including picolinamide's ability to inhibit poly(ADP-ribose) synthetase, thereby protecting against NAD depression,[61] picolinamide's increased radical scavenging abilities,[20] and nicotinamide's specific binding to certain proteins.[23]

In addition to the energetic differences, there are also significant differences in the entropies of activation for the amide bond rotation in picolinamide and nicotinamide. As the amide bond rotates into the transition state, there is a loss in the carbon−nitrogen bond order. The resulting increased density of states should lead to a positive entropy change in both cases. The concomitant increases in other bond orders, however, would likely keep the overall change in entropy small. A larger component of the entropy change is likely associated with the interaction of the amide protons with the solvent. For the protons pointing away from the pyridine ring, there are fewer steric restrictions on hydrogen bonding to the solvent molecules. In picolinamide the rotation is toward the pyridine ring, decreasing the available protons, while in nicotinamide, the rotation is away from the pyridine ring, providing an additional proton for hydrogen bonding to solvent molecules. This leads to a net entropy change for nicotinamide that is negative and a net entropy change for picolinamide that is small but positive. Similar entropy changes have been noted for other amide systems in hydrogen-bonding solvents.[1,9,15,60]

A remaining and subtle question concerns the observed difference in rotational barriers for the same molecule in different solvents and how the trends for picolinamide and nicotinamide are related to the differences in their transition state structures and charge distributions. Solvent effects have been observed in a number of amides and have been the subject of several theoretical investigations.[1,9,15] Given the error bars on the activation parameters in our data, solvent effects appear to be small. Overlaying the data, however, clearly shows that the molecules do behave differently in the nitrobenzene and pyridine solvents.

Concluding Remarks

Together, dynamic NMR and ab initio computational methods present a fairly detailed picture of the 5.4 kcal/mol difference in the amide rotational barriers for picolinamide and nicotinamide and quantify how amide bonds can be modified by a number of molecular factors. Proton chemical shifts and ab initio calculations of the scalar coupling confirm that picolinamide's potential is raised by an intramolecular hydrogen bond between the amide and pyridine ring. At the same time, nicotinamide's potential is lowered due to steric interactions in the ground state and superior π electron donation from the pyridine ring in the transition state. Interestingly, only a small amount of double bond character is lost in the ground state structure; the majority of the change in barrier in nicotinamide is due to superior resonance stabilization of the transition state compared to that for picolinamide.

Acknowledgment. This work was supported in part by NSF Grant CHE-9982362 and ACS PRF Grant 35320-G6 to L.J.M. R.A.O. is a Department of Education GAANN Fellow.

JA028751J

(60) Rablen, P. R.; Miller, D. A.; Bullock, V. R.; Hutchinson, P. H.; Gorman, J. A. *J. Am. Chem. Soc.* **1999**, *121*, 218−226.
(61) Morris, P. B.; Ellis, M.; Nixon, S. W. L. *J. Mol. Cell. Cardiol.* **1989**, *21*, 351−358.